THE JOURNAL OF PHYSICAL CHEMISTRY B

Article

pubs.acs.org/JPCB

Roles of Viscosity, Polarity, and Hydrogen-Bonding Ability of a Pyrrolidinium Ionic Liquid and Its Binary Mixtures in the Photophysics and Rotational Dynamics of the Potent Excited-State Intramolecular Proton-Transfer Probe 2,2′-Bipyridine-3,3′-diol

Sarthak Mandal, Surajit Ghosh, Chiranjib Banerjee, Jagannath Kuchlyan, and Nilmoni Sarkar*

Department of Chemistry, Indian Institute of Technology, Kharagpur 721302, West Bengal, India

Supporting Information

ABSTRACT: The room-temperature ionic liquid $[C_3mpyr][Tf_2N]$ and its binary mixtures with methanol and acetonitrile provide microenvironments of varying viscosity, polarity, and hydrogen-bonding ability. The present work highlights their effects on the photophysics and rotational dynamics of a potent excited-state intramolecular double-proton-transfer (ESIDPT) probe, 2,2′-bipyridine-3,3′-diol $[BP(OH)_2]$. The rotational diffusion of the proton-transferred diketo (DK) tautomer in $[C_3mpyr][Tf_2N]$ ionic liquid was analyzed for the first time from the experimentally obtained temperature-dependent fluorescence anisotropy data using Stokes−Einstein−Debye (SED) hydrodynamic theory and Gierer−Wirtz quasihydrodynamic theory (GW-QHT). It was found that the rotation of the DK tautomer in neat ionic liquid is governed solely by the viscosity of the medium, as the experimentally observed boundary-condition parameter, C_{obs}, was very close to the GW boundary-condition parameter (C_{GW}). On the basis of photophysical studies of $BP(OH)_2$ in IL−cosolvent binary mixtures, we suggest that methanol molecules form hydrogen bonds with the cationic counterpart of the DK tautomers, as evidenced by the greater extent of the decrease in the fluorescence lifetime of $BP(OH)_2$ upon addition of methanol compared to acetonitrile. It is also possible for the methanol molecules to form hydrogen bonds with the constituents of the RTIL, which is supported by the lesser extent of the decrease in the viscosity of the medium upon addition of methanol, leading to a less effective decrease in the rotational relaxation time compared to that observed upon acetonitrile addition.

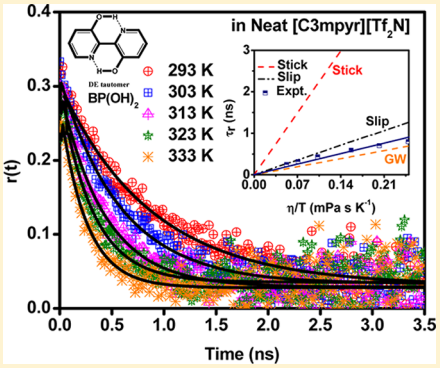

1. INTRODUCTION

Room-temperature ionic liquids (RTILs), which are molten salts at ambient temperature, have received a great deal of attention in recent years because of their unique physicochemical properties, such as negligible volatility, high electrochemical and thermal stability, and high ionic conductivity, which allow their use as green substitutes for volatile organic solvents in various applications.[1−5] More importantly, the desired properties of a solvent required for a particular application can be achieved with RTILs simply by changing the cationic and anionic constituents, and hence, RTILs are often called designer solvents. Extensive studies have been performed to gain a fundamental understanding of the physicochemical, electrochemical, and photochemical properties of various RTILs over the past few years,[6−8] and as a consequence, these RTILs are now being used in organic synthesis and catalysis, fabrication of inorganic materials, electrochemical studies, and many other chemical and technological applications.[9−13] The high viscosities of pure RTILs sometimes prevent their use in many chemical applications. However, their applicability can largely be enhanced by the addition of various organic cosolvents, such as water, methanol, and acetonitrile. Addition of a cosolvent leads to large changes in the polarity, viscosity, and ionic mobility (i.e., conductivity) of the medium.[14−17] Consequently, RTIL−cosolvent binary mixtures are an active topic of research aimed at gaining insight into the differences in their physicochemical properties from those of the neat ionic liquid. However, selection of the cosolvent is a key factor in obtaining the desired properties for a particular application. A number of theoretical, simulation, and experimental studies on the structures and dynamical behaviors of RTIL−cosolvent binary mixtures are available in the literature.[18−23]

Various spectroscopy-based photophysical and dynamical studies including excited-state proton transfer (ESPT), solvation dynamics, and photoinduced electron transfer (PET) have been performed over the past few years in RTILs and ionic liquids containing binary mixtures.[24−35] It has been found that the dynamics of such photoinduced processes in RTILs and RTIL−cosolvent binary mixtures are quite different from those observed in conventional solvents. As most of these studies have been performed on imidazolium-

Received: March 13, 2013
Revised: April 29, 2013
Published: May 13, 2013

 © 2013 American Chemical Society dx.doi.org/10.1021/jp4025443 | J. Phys. Chem. B 2013, 117, 6789−6800

Scheme 1. Different Phototautomers Involved in the ESIDPT Process of $BP(OH)_2$ Showing the Stepwise and Concerted Mechanisms

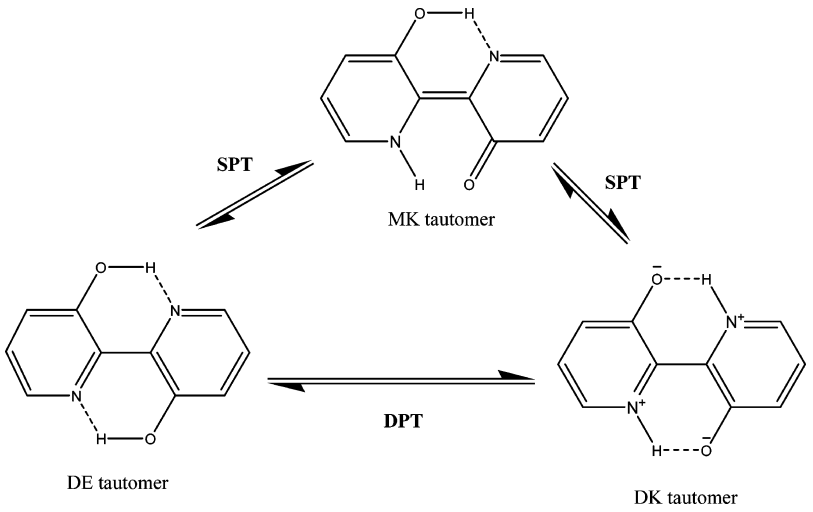

containing ionic liquids, studies on the photophysical properties of fluorophores in pyrrolidinium-containing ionic liquids are limited, particularly for dissolved solutes that exhibit excited-state intramolecular proton-transfer reactions. In the present work, we focus on the study of the photophysical properties of a potent excited-state intramolecular double-proton-transfer (ESIDPT) probe, 2,2′-bipyridine-3,3′-diol [$BP(OH)_2$], in a neat RTIL and its binary mixtures with organic cosolvents to elucidate the combined effects of the viscosity, polarity, and hydrogen-bonding ability of the surrounding medium. For this purpose, *N*-methyl-*N*-propylpyrrolidinium bis-[(trifluoromethyl)sulfonyl]imide (abbreviated as [C_3mpyr]-[Tf_2N]) was selected as the RTIL, and methanol and acetonitrile were chosen as the organic cosolvents. The choice of the cosolvents was motivated by the differential interactions of methanol and acetonitrile with the selected RTIL. Whereas methanol acts as both a hydrogen-bond donor and a hydrogen-bond acceptor, acetonitrile can act as only a weak hydrogen-bond acceptor.

2,2′-Bipyridine-3,3′-diol [$BP(OH)_2$] is a planar aromatic molecule that, upon photoexcitation, exhibits excited-state intramolecular double-proton transfer according to either a concerted or stepwise mechanism, as shown in Scheme 1. The proton-transfer (PT) reaction of this molecule has been well studied both experimentally[36−41] and theoretically.[42−44] The ESIDPT reaction through a concerted mechanism is reported to occur within a time scale of ∼100 fs.[45,46] However, in the sequential mechanism of the two-step process, the first step is reported to be ultrafast, with a time scale of about 100 fs or less, and the second step, which involves the formation of a diketo (DK*) tautomer from a monoketo (MK*) tautomer, occurs on a time scale of ∼10 ps. Several studies have indicated that the branching ratio of the PT reaction pathways (concerted/sequential) depends on the nature of the solvent and the excitation and emission wavelengths.[45,46] Marks et al.[47] studied the effects of solvent viscosity, polarity and hydrogen-bonding ability on the PT dynamics of $BP(OH)_2$ in a number of protic and aprotic solvents. Their results indicated that, in aprotic solvents, the ESIPT dynamics for the mono- to diketo conversion is not influenced by solvent properties such as polarity and viscosity or by temperature or deuteration of the solute. However, in protic solvents, the conversion rate is proportional to the viscosity coefficient of the solvent. Moreover, the PT dynamics of $BP(OH)_2$ has also been reported to be largely affected by the hydrogen-bonding abilities of protic solvents. Considering the high viscosities of RTILs, the ESIPT reaction rate for the conversion of the monoketo tautomer to the diketo tautomer of $BP(OH)_2$ in RTILs is expected to be significantly lower than that in conventional solvents. Moreover, it is also interesting to determine the influence of the addition of a small amount of cosolvent on the ESIPT dynamics of $BP(OH)_2$, as cosolvents are known to markedly affect the viscosity, polarity, and hydrogen-bonding ability of RTILs. Therefore, in this study, we investigated the effects of varying properties of RTILs and RTIL−cosolvent binary mixtures on the photophysical and dynamical behavior of $BP(OH)_2$.

Studying the photophysical properties of $BP(OH)_2$ is of particular interest not only because $BP(OH)_2$ is involved in the ESIDPT process but mainly because it is extremely sensitive to changes in the surrounding microenvironment, which allows $BP(OH)_2$ to be used in the study of protein conformations and binding-site polarities in various chemical and biological nanocavities.[48−58] Moreover, Abou-Zied[59] recently suggested that $BP(OH)_2$ can serve as a good mimic of a DNA base pair, similarly to a few other PT chromophores such as dimers of 7-azaindole.[60−62] Because most of the chemical, technological, and biomedical applications of ESIPT chromophores are based on their photophysical properties, great efforts have been made to study the photophysical properties of such molecules in various homogeneous and heterogeneous systems over the past few decades.[53−57,63,64] In neat solution, the large Stokes-shifted fluorescence of $BP(OH)_2$ is attributed to the zwitterionic DK tautomer. Both the dienol (DE) and diketo (DK) tautomers are reported to be nonpolar because they have negligible dipole moments in their first singlet excited states.[36,38] Therefore, both the absorption and fluorescence properties of $BP(OH)_2$ are expected to be slightly affected by changes in solvent polarity.[47] However, as the hydrogen-bonding ability of the solvent increases, the blue shift in the emission maximum increases.[54] Extensive studies have been performed on the photophysical properties of $BP(OH)_2$ in neat homogeneous solutions of varying pH, polarity, and hydrogen-bonding ability.[37,47,54,63,64] However, to the best of our knowledge, no such studies have

dx.doi.org/10.1021/jp4025443 | J. Phys. Chem. B 2013, 117, 6789−6800

yet been performed in RTILs and RTIL-containing binary solvent mixtures. Because the PT chromophore, $BP(OH)_2$, is reported to be highly sensitive to the surrounding microenvironment, especially to the hydrogen-bonding ability of the solvent, changes in the structure and dynamics of RTIL–cosolvent binary mixtures can be observed by photophysical techniques using $BP(OH)_2$ as a molecular reporter.

2. EXPERIMENTAL SECTION

2.1. Materials. 2,2′-Bipyridine-3,3′-diol [$BP(OH)_2$] was used as received from Sigma-Aldrich. *N*-Methyl-*N*-propylpyrrolidinium bis(trifluoromethanesulfonyl)imide ([C_3mpyr][Tf_2N]) was used as received without further purification as obtained from Kanto Chemical Co., Inc. (Tokyo, Japan). The molecular structure of the ionic liquid is given in Scheme 2. The organic cosolvents used, namely, methanol and acetonitrile, were of spectroscopic grade (Spectrochem, Mumbai, India).

Scheme 2. Molecular Structure of the Room-Temperature Ionic Liquid [C_3mpyr][Tf_2N]

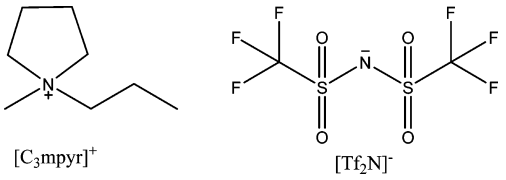

2.2. Preparation of Solutions. A stock solution of $BP(OH)_2$ was initially prepared in methanol. After that, a calculated amount of the stock methanolic solution was taken in a quartz cuvette so that the ultimate concentration of $BP(OH)_2$ became $\sim 10^{-5}$ M for a specific volume of solution. After complete removal of methanol, the requisite amount of RTIL was added to the cuvette under a nitrogen atmosphere, the cuvette was sealed with a septum and parafilm, and its contents were stirred for ~30 min. The requisite amount of cosolvent was added to the cuvette containing the RTIL, and the solution was mixed thoroughly and allowed to equilibrate for a sufficient time before each measurement. All experiments with addition of cosolvent were performed below the saturation solubility value of the cosolvents.

2.3. Instruments and Methods. Steady-state absorption and emission spectra were recorded on a Shimadzu (model UV 2450) UV–vis spectrophotometer and a Hitachi (model F-7000) spectrofluorimeter, respectively. Time-resolved fluorescence decay profiles were recorded using a time-correlated single-photon-counting (TCSPC) picosecond spectrometer. The detailed experimental setup for picosecond TCSPC was described in our previous publication.[65] In brief, a picosecond diode laser at 375 nm (NanoLED, IBH, Glasgow, U.K.) was used as the light source, and the signal was detected at the magic-angle (54.7°) polarization using a Hamamastsu microchannel plate (MCP) photomultiplier tube (PMT) (3809U). The typical instrument response function was 100 ps in our system. The decays were analyzed using IBH DAS-6 decay analysis software.

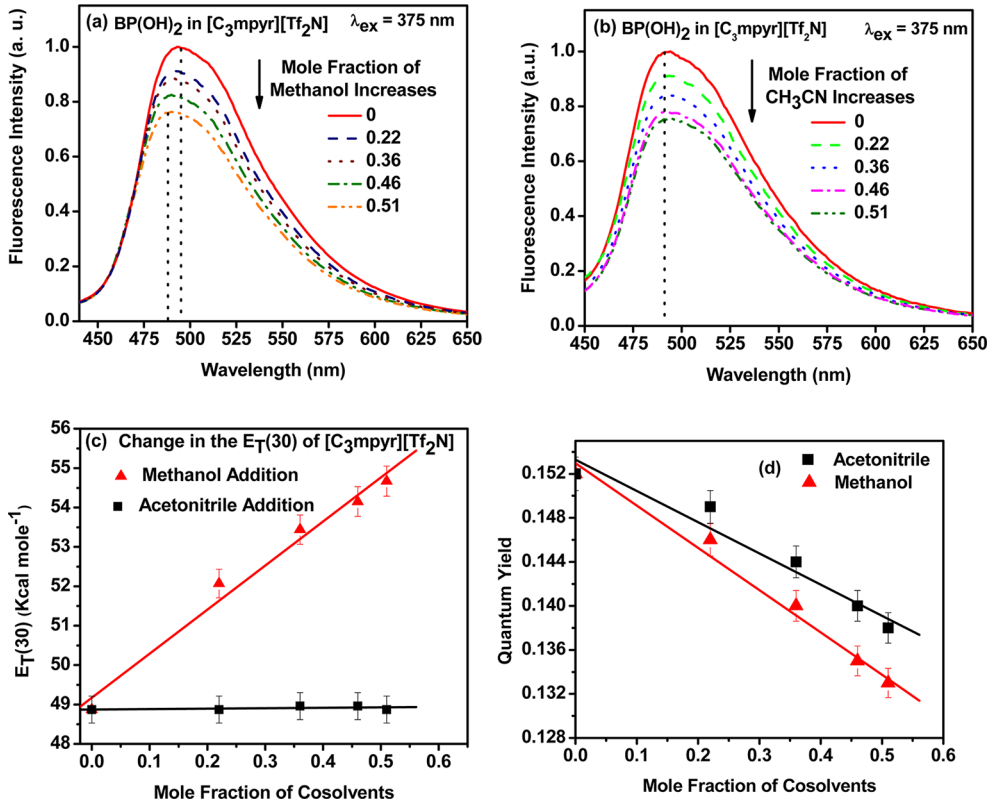

Figure 1. (a,b) Changes in the steady-state fluorescence spectra of $BP(OH)_2$ in [C_3mpyr][Tf_2N] with increasing mole fractions of (a) methanol and (b) acetonitrile, (c) changes in the polarity in terms of $E_T(30)$ values of the RTIL upon gradual addition of methanol and acetonitrile, and (d) changes in the fluorescence quantum yield of $BP(OH)_2$ in [C_3mpyr][Tf_2N] with increasing mole fractions of methanol and acetonitrile.

dx.doi.org/10.1021/jp4025443 | J. Phys. Chem. B 2013, 117, 6789–6800

Table 1. UV−Vis Absorption Maxima, Fluorescence Emission Maxima, Quantum Yields (Φ), and Decay Parameters of $BP(OH)_2$ in RTIL and RTIL−Cosolvent Binary Mixtures at 298 K

mole fraction of cosolvent	$E_T(30)$	λ_{max}^{abs} (nm)	λ_{max}^{emi} [a] (nm)	Φ	$\langle\tau\rangle_f$ [b] (ns)	k_r (10^8 s^{-1})	k_{nr} (10^8 s^{-1})	χ^2
				MeOH				
0	48.87	341	494	0.152	1.15	1.32	7.38	1.28
0.22	52.27	341	492	0.146	1.05	1.39	8.12	1.04
0.36	53.44	341	490	0.140	0.99	1.41	8.70	1.14
0.46	54.15	342	490	0.135	0.94	1.44	9.20	1.33
0.51	54.67	342	489	0.133	0.92	1.15	9.72	1.30
				CH_3CN				
0.22	48.87	341	494	0.149	1.07	1.39	7.95	1.20
0.36	48.96	342	494	0.144	1.03	1.40	8.31	1.28
0.46	48.96	342	494	0.140	1.00	1.40	8.60	1.14
0.51	48.87	341	494	0.138	0.99	1.39	8.71	1.29

[a]Experimental error = ±2 nm. [b]Average fluorescence lifetime (error limit = ±0.02 ns).

The same software was also used for time-resolved anisotropy decay analysis. For the anisotropy decays, we used a motorized polarizer on the emission side to collect the emission intensities at parallel ($I_\parallel$) and perpendicular ($I_\perp$) polarizations until a certain count difference between parallel ($I_\parallel$) and perpendicular ($I_\perp$) decay was reached, and the anisotropy decay function $r(t)$ was constructed from these $I_\parallel$ and $I_\perp$ decays using the equation

$$r(t) = \frac{I_\parallel(t) - GI_\perp(t)}{I_\parallel(t) + 2GI_\perp(t)} \quad (1)$$

where G is the instrument correction factor for detector sensitivity to the polarization of the emission. For our experimental setup, the value of the G factor at the detection wavelength was 0.6.

The fluorescence quantum yields of $BP(OH)_2$ in the RTIL and in its binary mixtures were determined using anthracene (λ_{ex} = 350 nm) with an absolute quantum yield of 0.27 in ethanol at 25 °C as a secondary standard[66] by means of the equation

$$\frac{\Phi_S}{\Phi_R} = \frac{A_S}{A_R}\frac{(Abs)_R}{(Abs)_S}\frac{{n_S}^2}{{n_R}^2} \quad (2)$$

where Φ represents the quantum yield, Abs represents the absorbance, A represents the area under the fluorescence curve, and n is the refractive index of the medium. The refractive index of the IL is 1.42, which was taken from the literature.[67] The refractive index values of the RTIL−cosolvent binary mixtures were determined theoretically using Lorentz−Lorenz equation as reported in the literature.[67] The subscripts S and R denote the corresponding parameters for the sample and reference, respectively.

2.4. Viscosity Measurements. Viscosities of the RTIL and RTIL−cosolvent binary mixtures were measured using a Brookfield DV-II+ Pro viscometer at 25 °C. We also determined the change in viscosity of the RTIL with changing temperature. The temperature was maintained constant by circulating water through the sample holder using a JEIO TECH Thermostat (RW-0525GS). The error limit of the instrument in the measurement of temperature is ±0.1 °C.

3. RESULTS AND DISCUSSIONS

3.1. Steady-State Studies. In neat $[C_3mpyr][Tf_2N]$, the absorption maximum of $BP(OH)_2$, which corresponds to the lowest (π,π^*) transition of the DE tautomer, appears at 340 nm, similarly to that appearing in all other conventional solvents.[54] Owing to the nonpolar nature of this tautomer with a negligible dipole moment, the position of the absorption maximum remained almost unchanged with the addition of cosolvents to neat $[C_3mpyr][Tf_2N]$ (Figure S1, Supporting Information). In aqueous solutions of $BP(OH)_2$, an additional absorption band at ∼400−450 nm is observed because of the stabilization of the DK tautomer in the ground state through formation of a hydrogen-bonding network with water molecules. No such additional absorption band was observed in the ionic liquid or ionic liquid−cosolvent binary mixtures, suggesting the nonexistence of the DK tautomer in the ground state in these solvents.

The steady-state fluorescence spectra of $BP(OH)_2$ in neat $[C_3mpyr][Tf_2N]$ and in $[C_3mpyr][Tf_2N]$ with gradual addition of the organic cosolvents methanol and acetonitrile were recorded at an excitation wavelength of 375 nm and are depicted in Figure 1a,b. In neat ionic liquid, $BP(OH)_2$ exhibits a fluorescence maximum at 494 nm, which is very close to the value obtained in acetonitrile (493 nm). Because of the symmetric nature of the DK tautomer, which has a negligible dipole moment, the emission maximum is expected to be only slightly affected with changing solvent polarity, as confirmed by the slight blue shift in the emission maximum of $BP(OH)_2$ in acetonitrile compared to that in the nonpolar solvent cyclohexane (λ_{max}^{emi} = 498 nm). However, the emission spectra of $BP(OH)_2$ are highly sensitive to the hydrogen-bonding ability of the surrounding microenvironment as a result of the formation of intermolecular hydrogen bonds through the rupture of intramolecular hydrogen bonds. This is further supported by the fact that the emission maximum of $BP(OH)_2$ is significantly blue-shifted in ethanol compared to that in acetonitrile, even though acetonitrile is reported to be more polar than ethanol.[54] With the addition of the polar protic solvent methanol to the ionic liquid, emission peak position therefore gradually blue-shifted and finally appeared at 489 nm after addition of 0.51 mol fraction of methanol. However, addition of acetonitrile did not lead to any change in the peak position. Therefore, the blue shift in the emission maximum upon the addition of methanol is clearly due to the change in the hydrogen-bonding ability of the binary mixture. A direct estimation of the polarity of this ionic liquid and the polarities of the IL−cosolvent binary mixtures was made from the absorption spectral data of a betaine 30 dye (Figure S2, Supporting Information), a well-known polarity probe.[68] The

dx.doi.org/10.1021/jp4025443 | J. Phys. Chem. B 2013, 117, 6789−6800

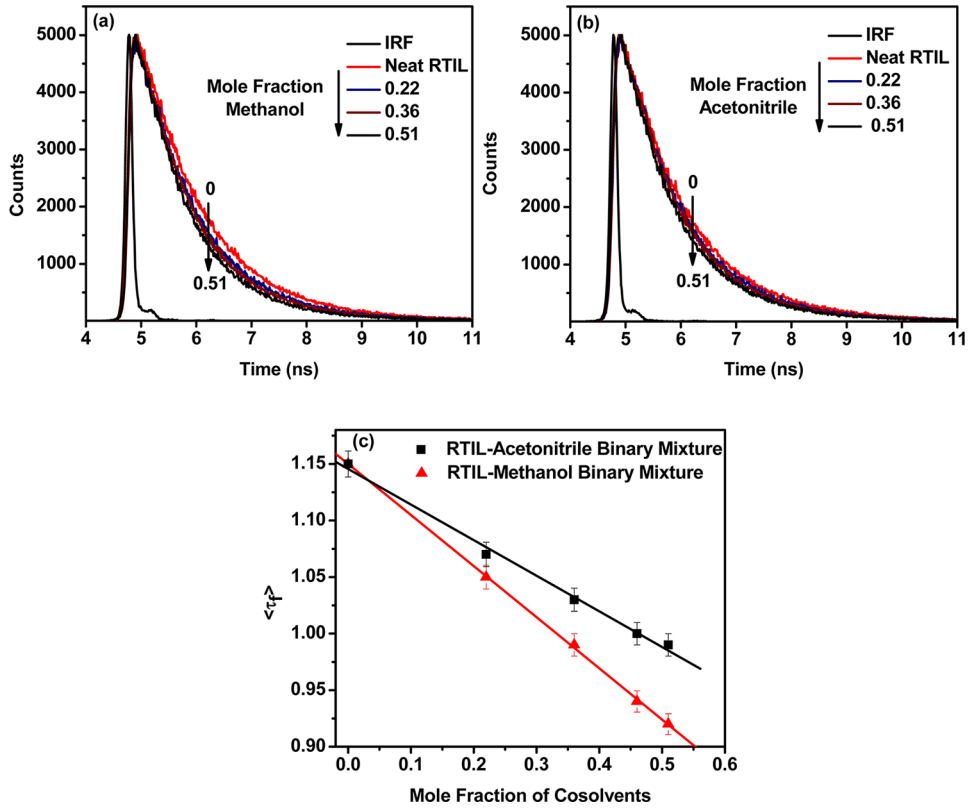

Figure 2. (a,b) Changes in the time-resolved fluorescence emission spectra (λ_{ex} = 375 nm) of $BP(OH)_2$ in $[C_3mpyr][Tf_2N]$ with increasing mole fractions of (a) methanol and (b) acetonitrile. (c) Dependence of the fluorescence lifetime on the mole fractions of different cosolvents: (▲) methanol and (■) acetonitrile.

$E_T(30)$ values were obtained from this method using the equation

$$E_T(30) = hc\nu_{max}N_A = \frac{28591}{\lambda_{max}\,(\text{nm})}\,\frac{\text{kcal}}{\text{mol}} \qquad (3)$$

where h, c, and N_A are Planck's constant, the velocity of light, and Avogadro's number, respectively. λ_{max} and ν_{max} are the wavelength (nm) and frequency, respectively, of the maximum absorption of the $E_T(30)$ probe. Figure 1c presents the changes in the $E_T(30)$ values of the ionic liquid with the addition of methanol and acetonitrile, as reported in Table 1. Currently, the change in the $E_T(30)$ value is considered to be a result of all types of possible specific and nonspecific interactions between the solvent and solute molecules. As one can see, the $E_T(30)$ value of neat $[C_3mpyr][Tf_2N]$ is 48.87, which is very close to the $E_T(30)$ value of acetonitrile (45.6). Addition of methanol resulted in an increase in the $E_T(30)$ value to 54.67 at 0.51 mol fraction of methanol mainly because of the increase in interactions, in particular hydrogen-bonding interactions, between the two concerned parties. However, we did not observe any significant change in the $E_T(30)$ value of the medium upon addition of acetonitrile, in complete agreement with that what we observed in steady-state fluorescence observations of $BP(OH)_2$ in $[C_3mpyr][Tf_2N]$–acetonitrile binary mixtures. In the cases of addition of both methanol and acetonitrile, the fluorescence quantum yield of $BP(OH)_2$ gradually decreased (Figure 1d). The extent of decrease in the quantum yield was more prominent for the addition of methanol as the cosolvent than for the addition of acetonitrile.

3.2. Time-Resolved Fluorescence Lifetime Measurements. Fluorescence lifetime measurements are necessary to obtain a clear idea about the excited-state interactions of the fluorophore with the surrounding medium. The time-resolved fluorescence decays of $BP(OH)_2$ in RTIL and IL–cosolvent binary mixtures were recorded at an excitation wavelength of 375 nm and monitored at their respective emission maxima, as shown in Figure 2a,b. In all cases, the decays fit well to a single-exponential function, and the fitted parameters are reported in Table 1. The measured fluorescence lifetime of $BP(OH)_2$ in neat $[C_3mpyr][Tf_2N]$ is 1.15 ns, which is very close to that in acetonitrile. This lifetime component is shorter, however, than that observed in nonpolar cyclohexane (3.10 ns).[54] This is basically due to the perturbation of the intramolecular hydrogen bonding through strong dipole–dipole interactions, especially the interaction of the anionic constituent of $[C_3mpyr][Tf_2N]$ with the cationic counterpart of the DK* tautomer, resulting in enhanced nonradiative decay channels of the proton-transferred tautomer in the excited state.

The lifetime further decreased upon the gradual addition of the cosolvents methanol and acetonitrile in $[C_3mpyr][Tf_2N]$. However, the extent of decrease was much more pronounced for the addition of methanol than for the addition of acetonitrile (Figure 2c), although methanol is reported to be less polar than acetonitrile. The reduction in fluorescence lifetime is consistent with the changes in the viscosity and hydrogen-bonding ability of the medium upon addition of cosolvent. Methanol can act as both a hydrogen-bond donor and acceptor. Therefore, the ability of this solvent to form hydrogen bonds through the rupture of intramolecular hydrogen bonds involved in the DK tautomer results in a more effective decrease in the fluorescence lifetime than for acetonitrile. This is an indication of the stronger excited-state

dx.doi.org/10.1021/jp4025443 | J. Phys. Chem. B 2013, 117, 6789–6800

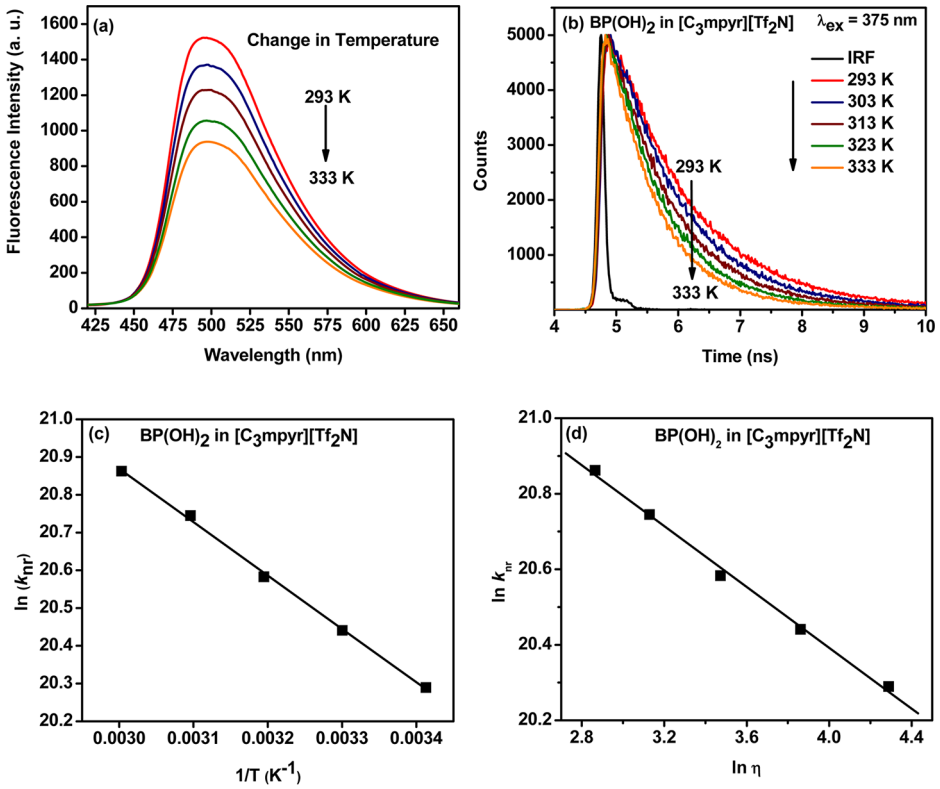

Figure 3. (a,b) Effects of temperature on (a) steady-state fluorescence spectra and (b) time-resolved fluorescence decays (λ_{ex} = 375 nm) of $BP(OH)_2$ in neat $[C_3mpyr][Tf_2N]$. (c,d) Plots of ln k_{nr} versus (c) $1/T$ and (d) ln η for $BP(OH)_2$ in neat $[C_3mpyr][Tf_2N]$ ionic liquid.

interaction of $BP(OH)_2$ with the $[C_3mpyr][Tf_2N]$–methanol mixture than the $[C_3mpyr][Tf_2N]$–acetonitrile mixture, and this can be explained by the larger change in the $E_T(30)$ value of the former solvent mixture as a result of all of the specific and nonspecific interactions between IL and methanol. All of the photophysical parameters, including the flurescence quantum yield (Φ_f), lifetime ($\langle\tau\rangle_f$), and radiative ($k_r = \Phi_f/\langle\tau\rangle_f$) and nonradiative ($k_{nr} = 1/\langle\tau\rangle_f - k_r$) decay rate constants of $BP(OH)_2$ in the neat RTIL and RTIL-containing mixed solvents are reported in Table 1.

We also determined the temperature dependency of the photophysical parameters by studying the fluorescence properties of $BP(OH)_2$ at different temperatures in the range of 283–333 K. With increasing temperature, both the steady-state fluorescence intensity and the fluorescence lifetime gradually decreased (Figure 3a,b, Table 2) in correlation with the decrease in bulk viscosity of $[C_3mpyr][Tf_2N]$, resulting in an enhanced nonradiative decay rate. However, it can be seen that, with an increase in temperature from 283 to 333 K, the nonradiative decay rate constant (k_{nr}) of $BP(OH)_2$ in the IL increased by only 1.8 times compared to the 4.2-times decrease in the bulk viscosity of $[C_3mpyr][Tf_2N]$. The activation energy for the nonradiative process in the neat RTIL was calculated from the slope of an Arrhenius plot of ln k_{nr} versus $1/T$ (Figure 3c), and the value of the activation energy was estimated as ~11.76 kJ/mol. This activation energy is associated with the energy barrier (E_0) of different intrinsic deactivation pathways and a solvent-dependent crossing barrier due to the viscosity of the medium. The nonradiative rate constant of a particular dye is related to the viscosity of the medium by the equation $k_{nr} \sim \eta^{-\alpha}$ where α is not a constant and varies strongly depending on the nature of the solvent. Here, we observed a linear plot of ln k_{nr} versus ln η (Figure 3d), and from the slope, we obtained a value of α = 0.40.

Table 2. Temperature-Dependent Fluorescence Decay Parameters of $BP(OH)_2$ in Neat $[C_3mpyr][Tf_2N]$

temperature	Φ	$\langle\tau\rangle_f$[a] (ns)	k_r (10^8 s^{-1})	k_{nr} (10^8 s^{-1})	χ^2
293	0.170	1.28	1.33	6.48	1.06
303	0.156	1.12	1.39	7.54	1.19
313	0.140	0.99	1.41	8.69	1.02
323	0.121	0.86	1.41	10.22	1.03
333	0.104	0.78	1.33	11.49	1.28

[a]Average fluorescence lifetime (error limit = ±0.02 ns).

3.3. Time-Resolved Fluorescence Anisotropy in RTIL–Cosolvent Binary Mixtures. Time-resolved fluorescence anisotropy measurements provide useful information regarding the rotational dynamics of the PT probe molecule. The fluorescence anisotropy decays of $BP(OH)_2$ in $[C_3mpyr][Tf_2N]$ and in its binary mixtures with methanol and acetonitrile fit well to a single-exponential function, and the fitted decay curves are shown in Figure 4a,b. The rotational relaxation time constant of $BP(OH)_2$ in $[C_3mpyr][Tf_2N]$ was found to be 0.70 ns at 25 °C (Table 3). Toele et al.[40] previously studied the femtosecond fluorescence anisotropy of $BP(OH)_2$ in acetonitrile and cyclohexane. They found an ultrafast anisotropy decay component of 350 fs that is attributed to the rotational motion of the dienol (DE*) tautomer. The additional picosecond components with time constants of 10 and 20–40 ps are responsible for the transformation of MK* to DK* and the rotational motion of the DK* in solution, respectively. However, in the present work, only the rotational motion of the relaxed excited-state species (DK*) generated

dx.doi.org/10.1021/jp4025443 | J. Phys. Chem. B 2013, 117, 6789–6800

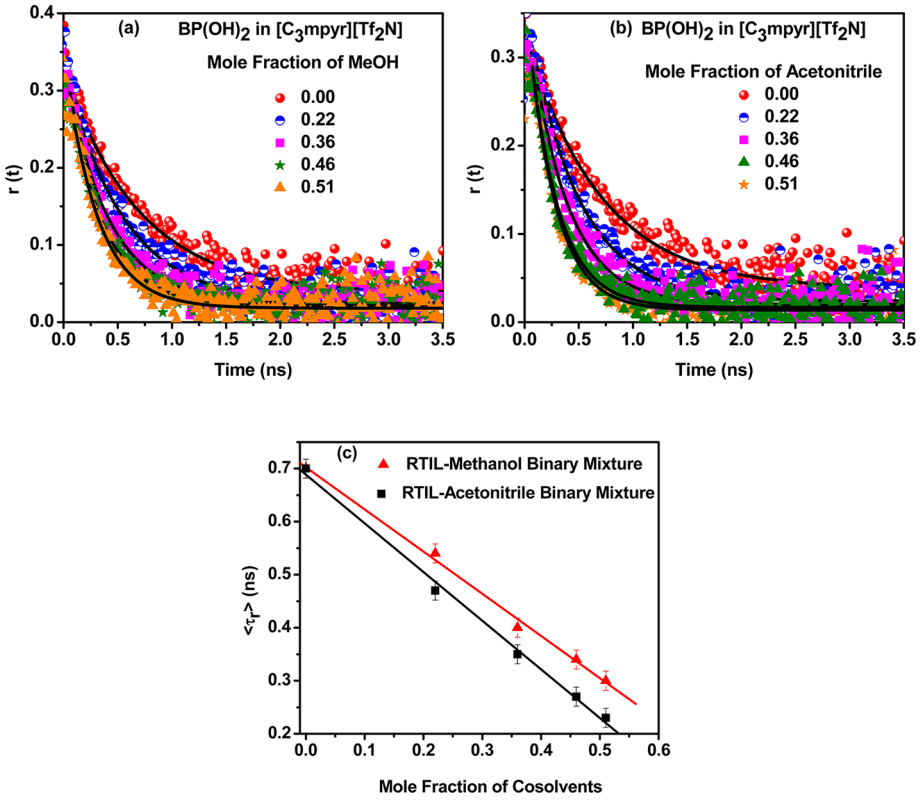

Figure 4. (a,b) Effects of gradual addition of (a) methanol and (b) acetonitrile on the fluorescence anisotropy decays (λ_{ex} = 375 nm, λ_{em} = 494 nm) of $BP(OH)_2$ in $[C_3mpyr][Tf_2N]$. (c) Dependence of the rotational relaxation time constant on the mole fractions of (▲) methanol and (■) acetonitrile.

Table 3. Rotational Relaxation Decay Parameters of $BP(OH)_2$ in RTIL and RTIL−Cosolvent Binary Mixtures

mole fraction of cosolvent	viscosity (cP)[a]	r_0[b]	$\langle\tau_r\rangle$ (ns)[c]	χ^2
	MeOH			
0	55.04	0.27	0.70	1.07
0.22	36.59	0.27	0.54	1.13
0.36	24.80	0.27	0.40	1.01
0.46	18.73	0.24	0.34	0.97
0.51	14.52	0.23	0.30	1.08
	CH_3CN			
0.22	30.19	0.27	0.47	0.96
0.36	18.54	0.26	0.35	0.96
0.46	11.07	0.27	0.27	0.98
0.51	9.42	0.26	0.26	1.00

[a]Error limit = ±5%. [b]Initial anisotropy. [c]Experimental error = ±0.01 ns.

after the ultrafast ESIDPT process is of primary interest as we report on the photophysical properties of $BP(OH)_2$ on the picosecond time scale. The higher rotational relaxation time (690 ps) in the RTIL compared to those in acetonitrile and cyclohexane (20−40 ps) can be rationalized on the basis of the high viscosity of the RTIL.

With the gradual addition of methanol and acetonitrile, the rotational relaxation time constant of the probe molecule decreased in both cases. The rotational relaxation time decreased from 0.69 to 0.30 ns upon addition of 0.51 mol fraction of methanol, whereas the addition of the same mole fraction of acetonitrile resulted in a decrease in the rotational relaxation time of $BP(OH)_2$ to 0.26 ns. Quantitatively, the rotational relaxation time of $BP(OH)_2$ decreased by ∼62% and ∼56% upon the addition of 0.51 mol fraction of acetonitrile and methanol, respectively, as cosolvents. The main reason behind the increase in the rotational motion (i.e., the decrease in rotational relaxation time) of the probe molecule upon addition of organic cosolvents is the decrease in viscosity of the medium. The viscosity of the ionic liquid is highly sensitive to the addition of organic cosolvents such as methanol and acetonitrile. The fact is that cosolvents decrease the aggregation of the constituent ions present in the ionic liquids, resulting in a decrease in the bulk viscosity of the medium. However, the nature of the cosolvent plays an important role in the magnitude of the decrease in viscosity. To understand the correlation between the decrease in the viscosity of the medium and the decrease in the rotational relaxation time constant, we measured the change in viscosity of $[C_3mpyr][Tf_2N]$ upon the gradual addition of cosolvents. The measured viscosities of the RTIL and the IL−cosolvent mixtures are reported in Table 3. The decrease in the rotational relaxation time upon addition of cosolvent was found to be well correlated with the decrease in the viscosity of the medium, as evidenced by the linear relationship between the bulk viscosity and the rotational relaxation time (Figure S3, Supporting Information). Our results suggest that, for the binary mixtures of $[C_3mpyr][Tf_2N]$ with methanol and acetonitrile, the decrease in viscosity, and hence, the decrease in rotational relaxation time of $BP(OH)_2$, is more prominent for the cosolvent acetonitrile, even though the dielectric constant of acetonitrile is higher than that of methanol (Figure 4c). The formation of hydrogen bonding between the anionic counterpart of the IL and methanol as predicted from the gas-phase theoretical calculations[24] could be one of the reasons for the lower decrease in viscosity upon

dx.doi.org/10.1021/jp4025443 | J. Phys. Chem. B 2013, 117, 6789−6800

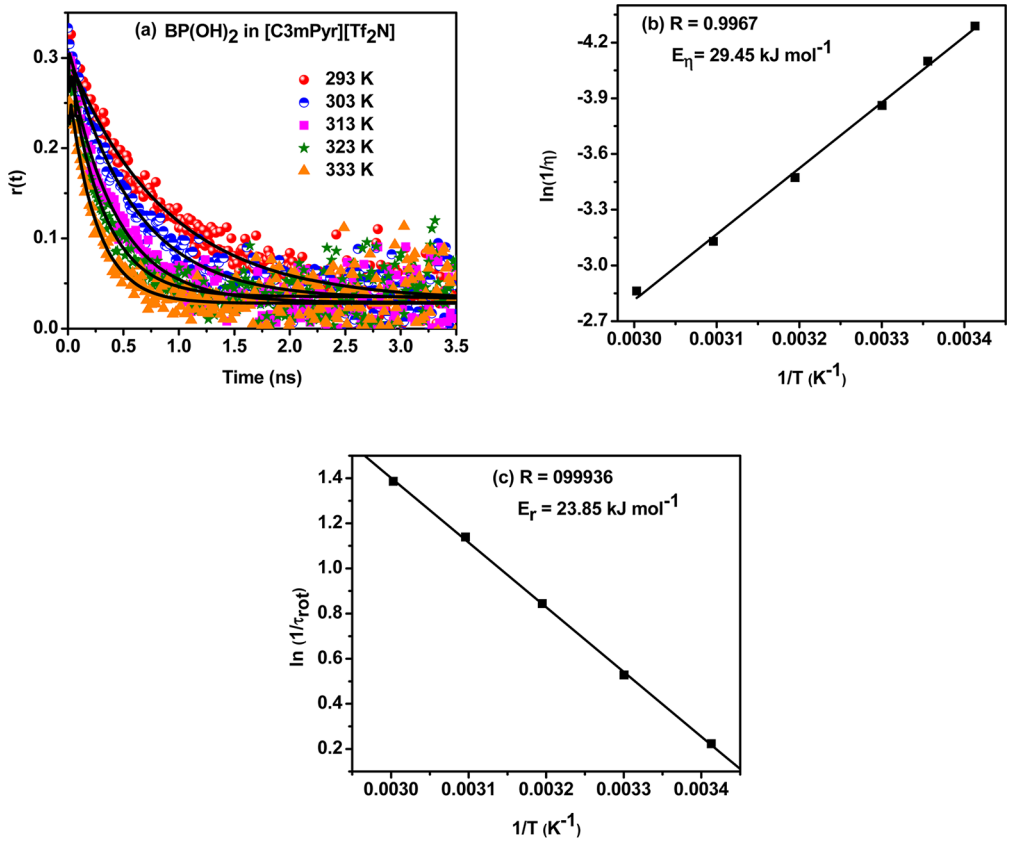

Figure 5. (a) Effects of temperature on the fluorescence anisotropy decays (λ_{ex} = 375 nm, λ_{em} = 494 nm) of $BP(OH)_2$ in $[C_3mpyr][Tf_2N]$. (b) Variation of the bulk viscosity of neat $[C_3mpyr][Tf_2N]$ with temperature (Arrhenius plot). (c) Effects of temperature on the rotational reorientation dynamics of $BP(OH)_2$ in neat $[C_3mpyr][Tf_2N]$ (Arrhenius plot).

addition of methanol than of acetonitrile. However, when both of the cosolvents are polar and protic, the decrease in viscosity is reported to be more prominent for the solvent with the lower dielectric constant. Fröba et al.[69] investigated the change in viscosity of the IL, $[C_2mim][C_2SO_4]$ with addition of cosolvent water and ethanol. They found that the decrease in viscosity is greater for the cosolvent with a lower dielectric constant.

3.4. Temperature-Dependent Rotational Diffusion of $BP(OH)_2$ in neat $[C_3mpyr][Tf_2N]$. In the recent literature,[70−78] there has been an increasing trend in the study of the rotational diffusion of neutral and charged molecules in room-temperature ionic liquids containing varying constituents using time-resolved fluorescence anisotropy measurements. Very recently, Guo et al.[78] investigated the rotational and translational dynamics of rhodamine 6G in a pyrrolidinium-containing ionic liquid using NMR spectroscopy and time-resolved fluorescence anisotropy measurements. In the present work, we measured the time-resolved fluorescence anisotropy decays of $BP(OH)_2$ in neat $[C_3mpyr][Tf_2N]$ at different temperatures ranging from 293 to 333 K. At each temperature, the anisotropy decays fit well to a single-exponential function, and the fitted curves and decay parameters are given in Figure 5a and Table 4, respectively. As can be seen, with increasing temperature, the rotational relaxation time decreased. The decrease in rotational relaxation time with increasing temperature is well correlated with the decrease in the bulk viscosity of the medium. To describe the temperature dependency of the viscosity, the activation energy for the viscous flow of $[C_3mpyr][Tf_2N]$ (i.e., the energy barrier for the movement of ions) was calculated from the slope of the Arrhenius plot of the

Table 4. Temperature-Dependent Fluorescence Anisotropy Decay Parameters of $BP(OH)_2$ in pure RTIL

temperature (K)	bulk viscosity[a] (cP)	r_0[b]	$\langle\tau_r\rangle$ (ns)[c]	χ^2
293	72.90	0.27	0.80	1.00
303	47.51	0.27	0.59	1.14
313	32.23	0.25	0.43	1.06
323	22.86	0.20	0.32	1.08
333	17.54	0.22	0.25	1.08

[a]Error limit = ±5%. [b]Initial anisotropy. [c]Experimental error = ±0.01 ns.

logarithmic form of $1/\eta$ versus $1/T$ (Figure 5b).[24] The activation energy (E_η) calculated for the viscous flow of $[C_3mpyr][Tf_2N]$ was 29.45 kJ/mol. Similarly, the activation energy for the rotational motion of $BP(OH)_2$ in $[C_3mpyr][Tf_2N]$ obtained from the Arrhenius plot of the logarithmic form of $1/\tau_r$ versus $1/T$ (Figure 5c) was found to be 23.86 kJ/mol. This value is very close to the activation barrier for the viscous flow of the RTIL. The results therefore indicate that the rotational relaxation motion of $BP(OH)_2$ is strictly guided by the viscosity of the medium without any major specific interactions.

To judge further whether any specific interactions are involved in the rotational motion of $BP(OH)_2$ in $[C_3mpyr][Tf_2N]$, the experimentally obtained reorientation times were further analyzed on the basis of the Stokes−Einstein−Debye (SED) hydrodynamic theory, as well as Gierer−Wirtz quasihydrodynamic theory (GW-QHT). These theoretical models have been extensively used over the past few years to

dx.doi.org/10.1021/jp4025443 | J. Phys. Chem. B 2013, 117, 6789−6800

explain the rotational diffusion of a number of polar and nonpolar solutes in RTILs.[70,73−75,77,78] According to the SED theory, the reorientation time of the probe molecule is related to the size and shape of the rotating molecule and also the viscosity (η) of the medium by the equation

$$\tau_r = \frac{VfC}{k_B}\left(\frac{\eta}{T}\right) \quad (4)$$

where V is the van der Waals volume of the solute, C is the boundary-condition parameter, f is the shape factor, and k_B is the Boltzmann constant. C represents the extent of coupling between the solute and solvent, and its value varies from 0 to 1 depending on the axial ratio of the solute molecule. The values 0 and 1 are the limits for hydrodynamic slip and stick boundary conditions, respectively. The stick boundary condition ($C = 1$) is always found to be valid for large particles. However, when the size of the solute is comparable to the size of the solvent molecules, the approximation of SED theory according to which the solvent is treated as a continuum begins to break down, and the slip boundary condition is gradually reached. It has been reported that, with increasing size of the solvent molecules, the solute molecules experience less friction.[71] In these cases, deviations between the experimentally obtained rotational reorientation times and the SED theory were observed. In the present work, we showed that the experimentally obtained rotational reorientation time of $BP(OH)_2$ in $[C_3mpyr][Tf_2N]$ ionic liquid deviates from the slip boundary condition of SED theory and follows subslip behavior because of the smaller size of $BP(OH)_2$ compared to the ionic liquid. The subslip behavior for the rotation of the probe molecule was successfully analyzed by using GW-QHT, which takes into account the relative sizes of the solvent and solute.

To calculate the reorientation time of $BP(OH)_2$ using SED hydrodynamic theory, the van der Waals volume of $BP(OH)_2$ was taken as 157 Å^3, which was estimated using Edward's volume increment method.[79] In SED hydrodynamic theory, the solute is assumed to be an asymmetric ellipsoid. Therefore, assuming $BP(OH)_2$ to be an ellipsoid, the axial radii a, b, and c are 5.8, 3.4, and 1.9 Å, respectively. The axes represent the distances of the long axis ($2a$), the short in-plane axis ($2b$), and the aromatic thickness ($2c$). Now, the diffusion coefficients D_i for the slip and stick boundary conditions were calculated from the friction coefficients ζ_i using the equation

$$D_i = \frac{kT}{\zeta_i} \quad (5)$$

The friction coefficients ζ_i with slip and stick boundary conditions were obtained from numerically tabulated values in the literature,[80,81] assuming that the dimensionless friction coefficients vary linearly from the tabulated values. The reorientation times within the limit of slip and stick boundary conditions can now be calculated using the equation

$$\tau_r = \frac{1}{12}\left(\frac{4D_a + D_b + D_c}{D_aD_b + D_bD_c + D_cD_a}\right) \quad (6)$$

where D_a, D_b, and D_c are the diffusion coefficients along the a, b, and c axes, respectively. From the reorientation times τ_r^{slip} and τ_r^{stick}, the calculated values of slip boundary-condition parameter (C_{slip}) and shape factor (f) for $BP(OH)_2$ are 0.24 and 1.88, respectively. These values are independent of temperature.

Figure 6 presents a plot of the experimentally measured τ_r values as a function of η/T for $BP(OH)_2$ along with the

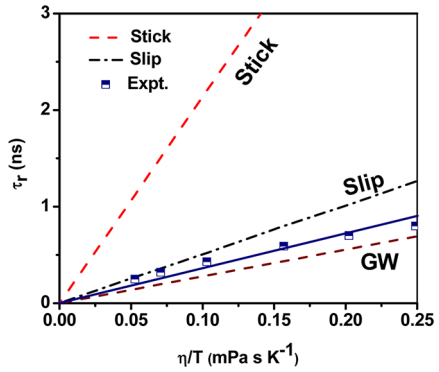

Figure 6. Plot of τ_r versus η/T for $BP(OH)_2$ in neat $[C_3mpyr][Tf_2N]$ ionic liquid. The lines passing through the experimental data points are drawn as visual aids. Theoretical reorientation times calculated using SED theory with slip, stick, and GW boundary conditions are also included.

theoretical obtained stick and slip boundary lines. From the figure, it is evident that the experimentally observed reorientation times of $BP(OH)_2$ in $[C_3mpyr][Tf_2N]$ ionic liquid follow subslip behavior. The fact that the rotational dynamics of $BP(OH)_2$ in $[C_3mpyr][Tf_2N]$ were faster than predicted by SED hydrodynamic slip boundary condition is not surprising, as the size of the ionic liquid (van der Waals volume calculated from Edward's increment method is 315 Å^3) is comparatively greater than the size of $BP(OH)_2$ (van der Walls volume = 157 Å^3). In such cases, SED hydrodynamic theory cannot satisfactorily account for the coupling between the solute and solvent molecules. The relative size effect of solvent and solute can be taken into account by Gierer−Wirtz quasihydrodynamic theory (GW-QHT).[70,82] The boundary condition C_{GW} can be obtained from the equations

$$C_{GW} = \sigma C_0 \quad (7)$$

$$\sigma = \frac{1}{1 + 6(V_S/V_P)^{1/3}C_0} \quad (8)$$

$$C_0 = \left\{\frac{6(V_S/V_P)^{1/3}}{[1 + 2(V_S/V_P)^{1/3}]^4} + \frac{1}{[1 + 4(V_S/V_P)^{1/3}]^3}\right\}^{-1} \quad (9)$$

where V_S and V_P are the van der Waals volumes of solvent and probe solute, respectively. The GW boundary-condition parameter (C_{GW}) thus obtained for $BP(OH)_2$ in $[C_3mpyr][Tf_2N]$ is 0.13, which is very close to the experimentally observed boundary-condition parameter ($C_{obs} = 0.18$), obtained from eq 4 by averaging the values at six different temperatures. Therefore, the GW model that incorporates the molecular sizes of the solvent and solute molecules can successfully explain the rotational motion of $BP(OH)_2$ in $[C_3mpyr][Tf_2N]$, as evidenced by the better agreement of the experimental data points shown in Figure 6.

4. CONCLUSIONS

In summary, the photophysical properties of $BP(OH)_2$ were studied for the first time in a pyrrolidinium-containing room-temperature ionic liquid and its binary mixtures with methanol

dx.doi.org/10.1021/jp4025443 | J. Phys. Chem. B 2013, 117, 6789−6800

and acetonitrile using steady-state and time-resolved fluorescence spectroscopy to understand the combined effects of viscosity, polarity, and hydrogen-bonding ability of the surrounding microenvironment. It was found that addition of a small amount of cosolvents in neat $[C_3mpyr][Tf_2N]$ resulted in a significant decrease in the fluorescence lifetime and rotational relaxation time of the dissolved probe molecules. However, acetonitrile was more effective in accelerating the rotational motion of the probe molecule than methanol, as the decrease in viscosity was more prominent for the addition of acetonitrile than methanol, even though the dielectric property of acetonitrile is greater than that of methanol. Moreover, with increasing temperature, the fluorescence lifetime and rotational relaxation time of $BP(OH)_2$ in $[C_3mpyr][Tf_2N]$ gradually decreased in correlation with the decrease in the viscosity of the medium with temperature. The rotational diffusion of the probe molecule was found to be governed solely by the viscosity of the medium, as confirmed by the comparable activation energy associated with the rotational motion of the probe molecules and the viscous flow of the ionic liquid. To further judge whether any specific interaction was operative in the system, the rotational dynamics of $BP(OH)_2$ in $[C_3mpyr][Tf_2N]$ ionic liquid was also studied using SED hydrodynamic theory and GW−quasihydrodynamic theory. It was observed that the reorientation times of $BP(OH)_2$ follow subslip behavior deviating from SED theory, which can be successfully explained using GW−quasihydrodynamic theory by taking into account the relative sizes of the solute and solvent molecules.

■ ASSOCIATED CONTENT

Ⓢ Supporting Information

Change in the absorption spectra and absorption spectra of the $E_T(30)$ probe upon the addition of cosolvents in neat ionic liquid and rotational relaxation time of $BP(OH)_2$ versus viscosity. This material is available free of charge via the Internet at http://pubs.acs.org.

■ AUTHOR INFORMATION

Corresponding Author

*E-mail: nilmoni@chem.iitkgp.ernet.in. Phone: +91-3222-283332.

Notes

The authors declare no competing financial interest.

■ ACKNOWLEDGMENTS

N.S. is thankful to Council of Scientific and Industrial Research (CSIR), Government of India, for a generous research grant. S.M. and S.G. are thankful to CSIR for research fellowships. C.B. and J.K. are thankful to UGC for research fellowships. We thank Dr. Moloy Sarkar (NISER Bhubaneswar, India) for helpful discussions.

■ REFERENCES

(1) El-Abedin, S. Z.; Endres, F. Ionic Liquids: The Link to High-Temperature Molten Salts? *Acc. Chem. Res.* **2007**, *40*, 1106−1113.
(2) Dupont, J. From Molten Salts to Ionic Liquids: A "Nano" Journey. *Acc. Chem. Res.* **2011**, *44*, 1223−1231.
(3) Rogers, R. D.; Seddon, K. R. Ionic Liquids—Solvents of the Future? *Science* **2003**, *302*, 792−793.
(4) Greaves, T. L.; Drummond, C. J. Protic Ionic Liquids: Properties and Applications. *Chem. Rev.* **2008**, *108*, 206−237.
(5) Castner, E. W., Jr.; Wishart, J. F. Spotlight on Ionic Liquids. *J. Chem. Phys.* **2010**, *132*, 120901−120909.
(6) Baker, G. A.; Baker, S. N.; Pandey, S.; Bright, F. V. An Analytical View of Ionic Liquids. *Analyst* **2005**, *130*, 800−808.
(7) Castner, E. W.; Wishart, J. F.; Shirota, H. Intermolecular Dynamics, Interactions, and Solvation in Ionic Liquids. *Acc. Chem. Res.* **2007**, *40*, 1217−1227.
(8) Hu, Z.; Margulis, C. J. Room-Temperature Ionic Liquids: Slow Dynamics, Viscosity, and the Red Edge Effect. *Acc. Chem. Res.* **2007**, *40*, 1097−1105.
(9) Hallett, J. P.; Welton, T. Room-Temperature Ionic Liquids: Solvents for Synthesis and Catalysis. 2. *Chem. Rev.* **2011**, *111*, 3508−3576.
(10) Pârvulescu, V. I.; Hardacre, C. Catalysis in Ionic Liquids. *Chem. Rev.* **2007**, *107*, 2615−2665.
(11) Bouvy, C.; Baker, G. A.; Yin, H.; Dai, S. Growth of Gold Nanosheets and Nanopolyhedra in Pyrrolidinium-Based Ionic Liquids: Investigation of the Cation Effect on the Resulting Morphologies. *Cryst. Growth Des.* **2010**, *10*, 1319−1322.
(12) Tsuda, T.; Hussey, C. L. Electrochemical Applications of Room Temperature Ionic Liquids. *Interface* **2007**, *16*, 42−49.
(13) Bhattacharyya, K. Room-Temperature Ionic Liquid: A Nanostructured Liquid for High-Vacuum and High-Energy Applications. *J. Phys. Chem. Lett.* **2010**, *1*, 3254−3255.
(14) Seddon, K. R.; Stark, A.; Torres, M. J. Influence of Chloride, Water, and Organic Solvents on the Physical Properties of Ionic Liquids. *Pure Appl. Chem.* **2000**, *72*, 2275−2287.
(15) Li, W.; Zhang, Z.; Han, B.; Hu, S.; Xie, Y.; Yang, G. Effect of Water and Organic Solvents on the Ionic Dissociation of Ionic Liquids. *J. Phys. Chem. B* **2007**, *111*, 6452−6456.
(16) Fletcher, K. A.; Pandey, S. Solvatochromic Probe Behavior within Ternary Room-Temperature Ionic Liquid 1-Butyl-3-methylimidazolium Hexafluorophosphate + Ethanol + Water Solutions. *J. Phys. Chem. B* **2003**, *107*, 13532−13539.
(17) Freire, M. G.; Neves, C. M. S. S.; Carvalho, P. J.; Gardas, R. L.; Fernandes, A. M.; Marrucho, I. M.; Santos, L. M. N. B. F.; Coutinho, J. A. P. Mutual Solubilities of Water and Hydrophobic Ionic Liquids. *J. Phys. Chem. B* **2007**, *111*, 13082−13089.
(18) Chaban, V. V.; Voroshylova, I. V.; Kalugin, O. N.; Prezhdo, O. V. Acetonitrile Boosts Conductivity of Imidazolium Ionic Liquids. *J. Phys. Chem. B* **2012**, *116*, 7719−7727.
(19) Chen, T.; Chidambaram, M.; Lin, Z. P.; Smit, B.; Bell, A. T. Viscosities of the Mixtures of 1-Ethyl-3-methylimidazolium Chloride with Water, Acetonitrile and Glucose: A Molecular Dynamics Simulation and Experimental Study. *J. Phys. Chem. B* **2010**, *114*, 5790−5794.
(20) Masaki, T.; Nishikawa, K.; Shirota, H. Microscopic Study of Ionic Liquid−H_2O Systems: Alkyl-Group Dependence of 1-Alkyl-3-methylimidazolium Cation. *J. Phys. Chem. B* **2010**, *114*, 6323−6331.
(21) Trivedi, S.; Pandey, S.; Baker, S. N.; Baker, G. A.; Pandey, S. Pronounced Hydrogen Bonding Giving Rise to Apparent Probe Hyperpolarity in Ionic Liquid Mixtures with 2,2,2-Trifluoroethanol. *J. Phys. Chem. B* **2012**, *116*, 1360−1369.
(22) Trivedi, S.; Malek, N. I.; Behera, K.; Pandey, S. Temperature-Dependent Solvatochromic Probe Behavior within Ionic Liquids and (Ionic Liquid + Water) Mixtures. *J. Phys. Chem. B* **2010**, *114*, 8118−8125.
(23) Annapureddy, H. V. R.; Hu, Z.; Xia, J.; Margulis, C. J. How Does Water Affect the Dynamics of the Room-Temperature Ionic Liquid 1-Hexyl-3-methylimidazolium Hexafluorophosphate and the Fluorescence Spectroscopy of Coumarin-153 When Dissolved in It? *J. Phys. Chem. B* **2008**, *112*, 1770−1776.
(24) Pramanik, R.; Rao, V. G.; Sarkar, S.; Ghatak, C.; Setua, P.; Sarkar, N. To Probe the Interaction of Methanol and Acetonitrile with the Ionic Liquid *N,N,N*-Trimethyl-*N*-propyl Ammonium Bis-(trifluoromethanesulfonyl) Imide at Different Temperatures by Solvation Dynamics Study. *J. Phys. Chem. B* **2009**, *113*, 8626−8634.
(25) Sarkar, S.; Mandal, S.; Ghatak, C.; Rao, V. G.; Ghosh, S.; Sarkar, N. Photoinduced Electron Transfer in an Imidazolium Ionic Liquid and in Its Binary Mixtures with Water, Methanol, and 2-Propanol:

Appearance of Marcus-Type of Inversion. *J. Phys. Chem. B* **2012**, *116*, 1335−1344.
(26) Das, A. K.; Mondal, T.; Sen, M. S.; Bhattacharyya, K. Marcus-like Inversion in Electron Transfer in Neat Ionic Liquid and Ionic Liquid-Mixed Micelles. *J. Phys. Chem. B* **2011**, *115*, 4680−4688.
(27) Sasmal, D. K.; Mandal, A. K.; Mondal, T.; Bhattacharyya, K. Diffusion of Organic Dyes in Ionic Liquid and Giant Micron Sized Ionic Liquid Mixed Micelle: Fluorescence Correlation Spectroscopy. *J. Phys. Chem. B* **2011**, *115*, 7781−7787.
(28) Liang, M.; Kaintz, A.; Baker, G. A.; Maroncelli, M. Bimolecular Electron Transfer in Ionic Liquids: Are Reaction Rates Anomalously High? *J. Phys. Chem. B* **2012**, *116*, 1370−1384.
(29) Paul, A.; Samanta, A. Solute Rotation and Solvation Dynamics in an Alcohol-Functionalized Room Temperature Ionic Liquid. *J. Phys. Chem. B* **2007**, *111*, 4724−4731.
(30) Bhattacharya, B.; Samanta, A. Excited-State Proton-Transfer Dynamics of 7-Hydroxyquinoline in Room Temperature Ionic Liquids. *J. Phys. Chem. B* **2008**, *112*, 10101−10106.
(31) Carlson, P. J.; Bose, S.; Armstrong, D. W.; Hawkins, T.; Gordon, M. S.; Petrich, J. W. Structure and Dynamics of the 1-Hydroxyethyl-4-amino-1,2,4-triazolium Nitrate High-Energy Ionic Liquid System. *J. Phys. Chem. B* **2012**, *116*, 503−512.
(32) Kimura, Y.; Fukuda, M.; Suda, K.; Terazima, M. Excited State Intramolecular Proton Transfer Reaction of 4′-*N*,*N*-Diethylamino-3-hydroxyflavone and Solvation Dynamics in Room Temperature Ionic Liquids Studied by Optical Kerr Gate Fluorescence Measurement. *J. Phys. Chem. B* **2010**, *114*, 11847−11858.
(33) Kimura, Y.; Hamamoto, T.; Terazima, M. Raman Spectroscopic Study on the Solvation of *N*,*N*-Dimethyl-*p*-nitroaniline in Room-Temperature Ionic Liquids. *J. Phys. Chem. A* **2007**, *111*, 7081−7089.
(34) Kashyap, H. K.; Biswas, R. Dipolar Solvation Dynamics in Room Temperature Ionic Liquids: An Effective Medium Calculation Using Dielectric Relaxation Data. *J. Phys. Chem. B* **2008**, *112*, 12431−12438.
(35) Kashyap, H. K.; Biswas, R. Solvation Dynamics of Dipolar Probes in Dipolar Room Temperature Ionic Liquids: Separation of Ion−Dipole and Dipole−Dipole Interaction Contributions. *J. Phys. Chem. B* **2010**, *114*, 254−268.
(36) Bulska, H. Intramolecular Cooperative Double Proton Transfer in [2,2′-Bipyridyl]-3,3′-diol. *Chem. Phys. Lett.* **1983**, *98*, 398−402.
(37) Sepiol, J.; Grabowska, A.; Bulska, H.; Mordzinski, A.; Perez Salgado, F.; Rettschnick, R. P. H. The Role of the Triplet State in Depopulation of the Electronically Excited Proton-Transferring System [2,2′-Bipyridy]l-3,3′-diol. *Chem. Phys. Lett.* **1989**, *163*, 443−448.
(38) Borowicz, P.; Grabowska, A.; Wortmann, R.; Liptay, W. Tautomerization in Fluorescent States of Bipyridyl-diols: A Direct Confirmation of the Intramolecular Double Proton Transfer by Electro-Optical Emission Measurements. *J. Lumin.* **1992**, *52*, 265−273.
(39) Marks, D.; Prosposito, P.; Zhang, H.; Glasbeek, M. Femtosecond Laser Selective Intramolecular Double-Proton Transfer in 2,2′-Bipyridyl-3,3′-diol. *Chem. Phys. Lett.* **1998**, *289*, 535−540.
(40) Toele, P.; Zhang, H.; Glasbeek, M. Femtosecond Fluorescence Anisotropy Studies of Excited-State Intramolecular Double-Proton Transfer in [2,2′-Bipyridyl]-3,3′-diol in Solution. *J. Phys. Chem. A* **2002**, *106*, 3651−3658.
(41) Zhang, H.; van der Meulen, P.; Glasbeek, M. Ultrafast Single and Double Proton Transfer in Photo-Excited [2,2′-Bipyridyl]-3,3′-diol. *Chem. Phys. Lett.* **1996**, *253*, 97−102.
(42) Ortiz-Sánchez, J. M.; Gelabert, R.; Moreno, M.; Lluch, J. M.; Anglada, J. M.; Bofill, J. M. Bipyridyl Derivatives as Photomemory Devices: A Comparative Electronic-Structure Study. *Chem.—Eur. J.* **2010**, *16*, 6693−6703.
(43) Barone, V.; Palma, A.; Sanna, N. Toward a Reliable Computational Support to the Spectroscopic Characterization of Excited State Intramolecular Proton Transfer: [2,2′-Bipyridine]-3,3′-diol as a Test Case. *Chem. Phys. Lett.* **2003**, *381*, 451−457.
(44) Plasser, F.; Barbatti, M.; Aquino, A. J. A.; Lischka, H. Excited-State Diproton Transfer in [2,2′-Bipyridyl]-3,3′-diol: The Mechanism Is Sequential, Not Concerted. *J. Phys. Chem. A* **2009**, *113*, 8490−8499.
(45) Prosposito, P.; Marks, D.; Zhang, H.; Glasbeek, M. Femtosecond Double Proton-Transfer Dynamics in [2,2′-Bipyridyl]-3,3′-diol in Sol−Gel Glasses. *J. Phys. Chem. A* **1998**, *102*, 8894−8902.
(46) Neuwahl, F. V. R.; Foggi, P.; Brown, R. G. Sub-Picosecond and Picosecond Dynamics in the S_1 State of [2,2′-Bipyridyl]-3,3′-diol Investigated by UV−Visible Transient Absorption Spectroscopy. *Chem. Phys. Lett.* **2000**, *319*, 157−163.
(47) Marks, D.; Zhang, H.; Glasbeek, M.; Borowicz, P.; Grabowska, A. Solvent Dependence of (Sub)Picosecond Proton Transfer in Photo-Excited [2,2′-Bipyridyl]-3,3′-diol. *Chem. Phys. Lett.* **1997**, *275*, 370−376.
(48) Zhong, D.; Douhal, A.; Zewail, A. H. Femtosecond Studies of Protein−Ligand Hydrophobic Binding and Dynamics: Human Serum Albumin. *Proc. Natl. Acad. Sci. U.S.A.* **2000**, *97*, 14056−14061.
(49) Catalán, J.; Valle, J. C. D.; Diaz, C.; Palomar, J.; Paz de, J. L. G.; Kasha, M. Solvatochromism of Fluorophores with an Intramolecular Hydrogen Bond and Their Use as Probes in Biomolecular Cavity Sites. *Int. J. Quantum Chem.* **1999**, *72*, 421−438.
(50) Douhal, A. Ultrafast Guest Dynamics in Cyclodextrin Nanocavities. *Chem. Rev.* **2004**, *104*, 1955−1976.
(51) Zhao, J.; Ji, S.; Chen, Y.; Guo, H.; Yang, P. Excited State Intramolecular Proton Transfer (ESIPT): From Principal Photophysics to the Development of New Chromophores and Applications in Fluorescent Molecular Probes and Luminescent Materials. *Phys. Chem. Chem. Phys.* **2012**, *14*, 8803−8817.
(52) Sytnik, A.; Gormin, D.; Kasha, M. Interplay between Excited-State Intramolecular Proton Transfer and Charge Transfer in Flavonols and Their Use as Protein-Binding-Site Fluorescence Probes. *Proc. Natl. Acad. Sci. U.S.A.* **1994**, *91*, 11968−11972.
(53) Abou-Zied, O. K. Investigating 2,2′-Bipyridine-3,3′-diol as a Microenvironment-Sensitive Probe: Its Binding to Cyclodextrins and Human Serum Albumin. *J. Phys. Chem. B* **2007**, *111*, 9879−9885.
(54) Abou-Zied, O. K. Steady-State and Time-Resolved Spectroscopy of 2,2′-Bipyridine-3,3′-diol in Solvents and Cyclodextrins: Polarity and Nanoconfinement Effects on Tautomerization. *J. Phys. Chem. B* **2010**, *114*, 1069−1076.
(55) Abou-Zied, O. K.; Al-Hinai, A. T. Caging Effects on the Ground and Excited States of 2,2′-Bipyridine-3,3′-diol Embedded in Cyclodextrins. *J. Phys. Chem. A* **2006**, *110*, 7835−7840.
(56) De, D.; Datta, A. Modulation of Ground- and Excited-State Dynamics of [2,2′-Bipyridyl]-3,3′-diol by Micelles. *J. Phys. Chem. B* **2011**, *115*, 1032−1037.
(57) Mandal, S.; Ghosh, S.; Aggala, H. H. K.; Banerjee, C.; Rao, V. G.; Sarkar, N. Modulation of the Photophysical Properties of 2,2′-Bipyridine-3,3′-diol inside Bile Salt Aggregates: A Fluorescence Based Study for the Molecular Recognition of Bile Salts. *Langmuir* **2013**, *29*, 133−143.
(58) Mandal, S.; Rao, V. G.; Ghatak, C.; Pramanik, R.; Sarkar, S.; Sarkar, N. Photophysics and Photodynamics of 1′-Hydroxy-2′-acetonaphthone (HAN) in Micelles and Nonionic Surfactants Forming Vesicles: A Comparative Study of Different Microenvironments of Surfactant Assemblies. *J. Phys. Chem. B* **2011**, *115*, 12108−12119.
(59) Abou-Zied, O. K. Examining [2,2′-Bipyridyl]-3,3′-diol as a Possible DNA Model Base Pair. *J. Photochem. Photobiol. A* **2006**, *182*, 192−201.
(60) Douhal, A.; Kim, S. K.; Zewail, A. H. Femtosecond Molecular Dynamics of Tautomerization in Model Base Pairs. *Nature* **1995**, *378*, 260−263.
(61) Smirnov, A. V.; English, D. S.; Rich, R. L.; Lane, J.; Teyton, L.; Schwabacher, A. W.; Luo, S.; Thornburg, R. W.; Petrich, J. W. Photophysics and Biological Applications of 7-Azaindole and Its Analogs. *J. Phys. Chem. B* **1997**, *101*, 2758−2769.
(62) Takeuchi, S.; Tahara, T. Femtosecond Ultraviolet−Visible Fluorescence Study of the Excited-State Proton-Transfer Reaction of 7-Azaindole Dimer. *J. Phys. Chem. A* **1998**, *102*, 7740−7753.
(63) Grabowska, A.; Borowicz, P.; Martire, D. O.; Braslavsky, S. E. Triplet States of Molecules Undergoing Internal Double-Proton

Transfer in the S_1 State: 2,2′-Bipyridyl-diol and Its 5,5′-Dimethylated Derivative. *Chem. Phys. Lett.* **1991**, *185*, 206−211.
(64) Rurack, K.; Hoffmann, K.; Al-Soufi, W.; Resch-Genger, U. 2,2′-Bipyridyl-3,3′-diol Incorporated into $AlPO_4$-5 Crystals and Its Spectroscopic Properties as Related to Aqueous Liquid Media. *J. Phys. Chem. B* **2002**, *106*, 9744−9752.
(65) Hazra, P.; Chakrabarty, D.; Sarkar, N. Solvation Dynamics of Coumarin 153 in Aqueous and Non-aqueous Reverse Micelles. *Chem. Phys. Lett.* **2003**, *371*, 553−562.
(66) Demasa, J. N.; Crosby, G. A. The Measurement of Photoluminescence Quantum Yields. A Review. *J. Phys. Chem.* **1971**, *75*, 991−1024.
(67) Seki, S.; Tsuzuki, S.; Hayamizu, K.; Umebayashi, Y.; Serizawa, N.; Takei, K.; Miyashiro, S. Comprehensive Refractive Index Property for Room-Temperature Ionic Liquids. *J. Chem. Eng. Data* **2012**, *57*, 2211−2216. Kurnia, K. A.; Taib, M. M.; Mutalib, M. I. A.; Murugesan, T. Densities, Refractive Indices and Excess Molar Volumes for Binary Mixtures of Protic Ionic Liquids with Methanol at T = 293.15 to 313.15 K. *J. Mol. Liq.* **2011**, *159*, 211−219.
(68) Reichardt, C. Solvatochromic Dyes as Solvent Polarity Indicators. *Chem. Rev.* **1994**, *94*, 2319−2358.
(69) Fröba, A. P.; Wasserscheid, P.; Gerhard, D.; Kremer, H.; Leipertz, A. Revealing the Influence of the Strength of Coulomb Interactions on the Viscosity and Interfacial Tension of Ionic Liquid Cosolvent Mixtures. *J. Phys. Chem. B* **2007**, *111*, 12817−12822.
(70) Dutta, G. B. Influence of Specific Interactions on the Rotational Dynamics of Charged and Neutral Solutes in Ionic Liquids Containing Tris(pentafluoroethyl)trifluorophosphate (FAP) Anion. *J. Phys. Chem. B* **2010**, *114*, 8971−8977.
(71) Sachdeva, A.; Dutt, G. B. Temperature-Dependent Rotational Relaxation in a Viscous Alkane: Interplay of Shape Factor and Boundary Condition on Molecular Rotation. *J. Chem. Phys.* **2003**, *118*, 8307−8314.
(72) Karve, L.; Dutt, G. B. Rotational Diffusion of Neutral and Charged Solutes in Ionic Liquids: Is Solute Reorientation Influenced by the Nature of the Cation? *J. Phys. Chem. B* **2011**, *115*, 725−729.
(73) Karve, L.; Dutt, G. B. Role of Specific Interactions on the Rotational Diffusion of Organic Solutes in a Protic Ionic Liquid−Propylammonium Nitrate. *J. Phys. Chem. B* **2012**, *116*, 9107−9113.
(74) Das, S. K.; Sarkar, M. Rotational Dynamics of Coumarin-153 and 4-Aminophthalimide in 1-Ethyl-3-methylimidazolium Alkylsulfate Ionic Liquids: Effect of Alkyl Chain Length on the Rotational Dynamics. *J. Phys. Chem. B* **2012**, *116*, 194−202.
(75) Das, S. K.; Sarkar, M. Studies on the Solvation Dynamics of Coumarin 153 in 1-Ethyl-3-methylimidazolium Alkylsulfate Ionic Liquids: Dependence on Alkyl Chain Length. *ChemPhysChem* **2012**, *13*, 2761−2768.
(76) Das, S. K.; Sarkar, M. Solvation and Rotational Relaxation of Coumarin 153 and 4-Aminophthalimide in a New Hydrophobic Ionic Liquid: Role of N−H···F Interaction on Solvation Dynamics. *Chem. Phys. Lett.* **2011**, *515*, 23−28.
(77) Das, S. K.; Sahu, P. K.; Sarkar, M. Diffusion−Viscosity Decoupling in Solute Rotation and Solvent Relaxation of Coumarin153 in Ionic Liquids Containing Fluoroalkylphosphate (FAP) Anion: A Thermophysical and Photophysical Study. *J. Phys. Chem. B* **2013**, *117*, 636−647.
(78) Guo, J.; Han, K. S.; Mahurin, S. M.; Baker, G. A.; Hillesheim, P. C.; Dai, S.; Hagaman, E. W.; Shaw, R. W. Rotational and Translational Dynamics of Rhodamine 6G in a Pyrrolidinium Ionic Liquid: A Combined Time-Resolved Fluorescence Anisotropy Decay and NMR Study. *J. Phys. Chem. B* **2012**, *116*, 7883−7890.
(79) Edward, J. T. Molecular Volumes and the Stokes−Einstein Equation. *J. Chem. Educ.* **1970**, *47*, 261−270.
(80) Sension, R. J.; Hochstrasser, R. M. Comment on: Rotational Friction Coefficients for Ellipsoids and Chemical Molecules with Slip Boundary Conditions. *J. Chem. Phys.* **1993**, *98*, 2490−2490.
(81) Small, E. W.; Isenberg, I. Hydrodynamic Properties of a Rigid Molecule: Rotational and Linear Diffusion and Fluorescence Anisotropy. *Biopolymers* **1977**, *16*, 1907−1928.
(82) Fruchey, K.; Fayer, M. D. Dynamics in Organic Ionic Liquids in Distinct Regions Using Charged and Uncharged Orientational Relaxation Probes. *J. Phys. Chem. B* **2010**, *114*, 2840−2845.